

 Open access • Journal Article • DOI:10.1063/1.4923356

Sensitivity study of multi-layer active magnetic regenerators using first order magnetocaloric material $\text{La}(\text{Fe},\text{Mn},\text{Si})_{13}\text{Hy}$ — [Source link](#)

Tian Lei, Kaspar Kirstein Nielsen, Kurt Engelbrecht, Christian R.H. Bahl ...+2 more authors

Institutions: Technical University of Denmark, University of Southern Denmark

Published on: 06 Jul 2015 - Journal of Applied Physics (AIP Publishing)

Topics: Curie temperature and Magnetic refrigeration

Related papers:

- [The performance of a large-scale rotary magnetic refrigerator](#)
- [Experimental comparison of multi-layered La–Fe–Co–Si and single-layered Gd active magnetic regenerators for use in a room-temperature magnetic refrigerator](#)
- [Materials Challenges for High Performance Magnetocaloric Refrigeration Devices](#)
- [Magnetocaloric Energy Conversion](#)
- [Magnetic refrigeration : Single and multimaterial active magnetic regenerator experiments](#)

Share this paper:    

View more about this paper here: <https://typeset.io/papers/sensitivity-study-of-multi-layer-active-magnetic-2zfg4xdbea>



University of Southern Denmark

Sensitivity Study of Multi-layer Active Magnetic Regenerators Using First Order Magnetocaloric Material $\text{La}(\text{Fe},\text{Si},\text{Mn})_{13}\text{H}_y$

Lei, Tian; K. Nielsen, Kaspar; Engelbrecht, Kurt ; Bahl, Christian; Bez, Henrique Neves; Veje, Christian

Published in:
Journal of Applied Physics

DOI:
10.1063/1.4923356

Publication date:
2015

Document version:
Final published version

Citation for polished version (APA):

Lei, T., K. Nielsen, K., Engelbrecht, K., Bahl, C., Bez, H. N., & Veje, C. (2015). Sensitivity Study of Multi-layer Active Magnetic Regenerators Using First Order Magnetocaloric Material $\text{La}(\text{Fe},\text{Si},\text{Mn})_{13}\text{H}_y$. *Journal of Applied Physics*, 118(1), [014903]. <https://doi.org/10.1063/1.4923356>

Go to publication entry in University of Southern Denmark's Research Portal

Terms of use

This work is brought to you by the University of Southern Denmark.
Unless otherwise specified it has been shared according to the terms for self-archiving.
If no other license is stated, these terms apply:

- You may download this work for personal use only.
- You may not further distribute the material or use it for any profit-making activity or commercial gain
- You may freely distribute the URL identifying this open access version

If you believe that this document breaches copyright please contact us providing details and we will investigate your claim.
Please direct all enquiries to puresupport@bib.sdu.dk

Sensitivity study of multi-layer active magnetic regenerators using first order magnetocaloric material $\text{La}(\text{Fe},\text{Mn},\text{Si})_{13}\text{H}_y$

Tian Lei, Kaspar K. Nielsen, Kurt Engelbrecht, Christian R. H. Bahl, Henrique Neves Bez, and Christian T. Veje

Citation: *Journal of Applied Physics* **118**, 014903 (2015);

View online: <https://doi.org/10.1063/1.4923356>

View Table of Contents: <http://aip.scitation.org/toc/jap/118/1>

Published by the [American Institute of Physics](#)

Articles you may be interested in

[Specific heat and entropy change at the first order phase transition of \$\text{La}\(\text{Fe-Mn-Si}\)_{13}\text{-H}\$ compounds](#)

Journal of Applied Physics **118**, 053907 (2015); 10.1063/1.4928086

[Enhanced mechanical properties and large magnetocaloric effects in bonded \$\text{La}\(\text{Fe}, \text{Si}\)_{13}\$ -based magnetic refrigeration materials](#)

Applied Physics Letters **104**, 062407 (2014); 10.1063/1.4865236

[Selective laser melting of \$\text{La}\(\text{Fe},\text{Co},\text{Si}\)_{13}\$ geometries for magnetic refrigeration](#)

Journal of Applied Physics **114**, 043907 (2013); 10.1063/1.4816465

[Strain development during the phase transition of \$\text{La}\(\text{Fe},\text{Mn},\text{Si}\)_{13}\text{H}_2\$](#)

Applied Physics Letters **109**, 051902 (2016); 10.1063/1.4960358

[Heat exchangers made of polymer-bonded \$\text{La}\(\text{Fe},\text{Si}\)_{13}\$](#)

Journal of Applied Physics **115**, 17A941 (2014); 10.1063/1.4868707

[Mechanical properties and magnetocaloric effects in \$\text{La}\(\text{Fe}, \text{Si}\)_{13}\$ hydrides bonded with different epoxy resins](#)

Journal of Applied Physics **117**, 063902 (2015); 10.1063/1.4908018

Scilight

Sharp, quick summaries **illuminating**
the latest physics research

Sign up for **FREE!**

AIP
Publishing

Sensitivity study of multi-layer active magnetic regenerators using first order magnetocaloric material $\text{La}(\text{Fe},\text{Mn},\text{Si})_{13}\text{H}_y$

Tian Lei,^{1,a)} Kaspar K. Nielsen,¹ Kurt Engelbrecht,¹ Christian R. H. Bahl,¹ Henrique Neves Bez,¹ and Christian T. Veje²

¹Department of Energy Conversion and Storage, Technical University of Denmark, Frederiksborgvej 399, DK 4000 Roskilde, Denmark

²Mærsk Mc-Kinney Møller Institut, University of Southern Denmark, DK 5230 Odense M, Denmark

(Received 27 February 2015; accepted 21 June 2015; published online 6 July 2015)

We present simulation results of multi-layer active magnetic regenerators using the solid-state refrigerant $\text{La}(\text{Fe},\text{Mn},\text{Si})_{13}\text{H}_y$. This material presents a large, however quite sharp, isothermal entropy change that requires a careful choice of number of layers and working temperature for multi-layer regenerators. The impact of the number of layers and the sensitivity to the working temperature as well as the temperature span are quantified using a one dimensional numerical model. A study of the sensitivity of variation in Curie temperature through a uniform and normal distribution is also presented. The results show that the nominal cooling power is very sensitive to the Curie temperature variation in the multi-layer regenerators. A standard deviation of the Curie temperature variation for a normal distribution less than 0.6 K is suggested in order to achieve sufficient performance of a 15-layer regenerator with Curie temperature spacing of 2 K. © 2015 AIP Publishing LLC.

[<http://dx.doi.org/10.1063/1.4923356>]

I. INTRODUCTION

Magnetic refrigeration is a promising technology compared to vapor-compression systems due to the use of environmentally friendly heat transfer fluids and solid-state refrigerants, as well as a potentially high efficiency. With various improvements in magnetocaloric materials (MCMs), system design, and fluid control, the magnetic refrigeration technique has recently undergone a rapid development and several kilowatt class prototypes have emerged.^{1,2} MCMs exhibit a temperature rise due to adiabatic magnetization, or temperature decrease when adiabatically demagnetized. The magnetocaloric effect has a peak near the Curie temperature T_C of the MCM, and T_C is the temperature at which the transition from ferro- to paramagnetic phase takes place. With permanent magnets producing fields on the order of 1.5 T, the adiabatic temperature change of the best performing material will be about 5 K,³ which may not be sufficient for practical applications. To achieve a large temperature span, the concepts of active magnetic regeneration (AMR)⁴ and multi-layer regenerators are widely used in the design of existing machines.^{2,5,6} An AMR regenerator has a similar porous structure and oscillating flow pattern as some passive regenerative heat exchangers, but uses the MCM to transfer magnetic work into the regenerator, allowing it to absorb a cooling power over a useful temperature span.

A typical AMR cycle⁷ starts from the adiabatic magnetization process, which causes the solid temperature to increase. Then the heat transfer fluid flows through the porous bed from the cold to the hot end and is heated by the solid. At the hot end, the fluid rejects excess heat to the ambient. Followed by the adiabatic demagnetization and a temperature

decrease of the MCM, the hot-to-cold flow will reject heat to the solid and reach a lower temperature than the initial condition. Then the fluid absorbs heat, i.e., a cooling load, at the cold end. After several cycles, a temperature gradient is achieved along the axial direction and the regenerator reaches a periodic steady state. The net enthalpy flows at the ends are the heating and cooling power (Q_h and Q_c), respectively.

The material's performance has significant effect on the cooling power and the regenerator efficiency. Recent research has presented various interesting materials with compelling performance,^{2,6,8} especially, MCMs with a first-order phase transition at the Curie temperature have a large isothermal entropy change ΔS_{mag} . It is defined as

$$\Delta S_{mag}(T, H_i : H_f) \equiv S(T, H_f) - S(T, H_i), \quad (1)$$

with H and T denoting magnetic field and temperature, respectively, and the subscripts i and f denoting initial and final state, respectively. The isothermal entropy change of these first-order transition materials is often large compared to MCMs with a pure second order transition like gadolinium (Gd). $\text{La}(\text{Fe},\text{Mn},\text{Si})_{13}\text{H}_y$ is an attractive first order material and is subject to extensive research due to the high values of ΔS_{mag} , a small hysteresis effect, adjustable T_C , relatively high thermal conductivity, and high stability.^{9–11} The material was developed from $\text{La}(\text{Fe}_x\text{Si}_{1-x})_{13}$, where the Curie temperature can be tuned by the addition of hydrogen.¹² Barcza *et al.*¹⁰ pointed out that it is difficult to control partial hydrogenation on the industrial level with high accuracy; therefore, a method of substituting Fe with Mn¹³ was used. With this method, the material is always fully hydrogenated while the Mn content tunes T_C .

Although it is anticipated that large ΔS_{mag} will improve the regenerator performance, it decreases quickly at temperatures away from its T_C . A sharp peak may prevent the

^{a)}Electronic mail: tile@dtu.dk

material from working in the optimal temperature region. Multi-layer regenerators, in which each layer is aligned to make sure the T_C of each material follows the temperature gradient, can be a solution to this issue. Larger temperature spans as well as cooling capacities are expected in multi-layer regenerators using first order materials compared to single-material regenerators.

Smith *et al.*¹⁴ pointed out that for first order materials, the peak in the specific heat will move significantly with the applied field, and in reality the ΔS_{mag} peaks also show similar shift to higher temperature in a high applied field.¹¹ It is implied that the best working temperature for the first order material is expected to be higher than the Curie temperature. Therefore, multi-layer regenerators could be sensitive to the working temperature and a study of how a regenerator bed should be layered is therefore presented here.

Moreover, it may be difficult to control the T_C of each material to a high accuracy when fabricating a layered regenerator. Actual regenerator beds will have some arrangements in which T_C deviates from the intended design. This paper investigates how random variations in T_C affect the AMR performance. First, the impact of the Curie temperature variation of a single layer in each position is investigated. Then a more general study is carried out, where each layer in the regenerator deviates from the desired T_C according to either a uniform distribution or a normal distribution with a set standard deviation σ .

II. ONE DIMENSIONAL NUMERICAL MODEL OF AMR

A one-dimensional transient numerical model for simulating the AMR regenerators has been developed based on the work presented by Engelbrecht *et al.*⁸ The energy equations for the fluid and solid in the transient model^{8,15} can be written as

$$\frac{\partial}{\partial x} \left(k_{disp} A_c \frac{\partial T_f}{\partial x} \right) - \dot{m} c_f \frac{\partial T_f}{\partial x} - \frac{Nu k_f}{d_h} a_s A_c (T_f - T_r) + \left| \frac{\partial P}{\partial x} \frac{\dot{m}}{\rho_f} \right| = \rho_f A_c \varepsilon c_f \frac{\partial T_f}{\partial t}, \quad (2)$$

$$\frac{Nu k_f}{d_h} a_s A_c (T_f - T_r) + \frac{\partial}{\partial x} \left(k_{stat} A_c \frac{\partial T_r}{\partial x} \right) + (1 - \varepsilon) A_c \rho_r T_r \left(\frac{\partial s_r}{\partial H} \right)_T \frac{\partial H}{\partial t} = \rho_r (1 - \varepsilon) A_c c_{r,H} \frac{\partial T_r}{\partial t}, \quad (3)$$

where k , T , ρ , c , and s are the thermal conductivity, temperature, density, specific heat, and specific entropy; A_c , d_h , a_s , and ε are the cross section area, hydraulic diameter, specific area, and porosity, which reflect the geometry characteristics of a regenerator; x , t , \dot{m} , and H are the axial position, time, mass flow rate, and internal magnetic field. The subscripts f and r represent fluid and solid refrigerant, respectively. More details for the expressions of thermal conductivity due to fluid dispersion k_{disp} , static thermal conductivity k_{stat} , pressure drop $\frac{\partial P}{\partial x}$, and Nusselt number Nu are presented by Nielsen *et al.*¹⁶ It should be noted that k_{disp} and k_{stat} are already scaled to fit the cross-sectional area; therefore, the

porosity is not included in the conduction terms. From left to right in the fluid energy equation, the thermal dispersion, convection, heat transfer between solid and fluid, viscous dissipation, and energy storage are considered; the terms for the energy equation of the solid side are the heat transfer between solid and fluid, axial heat conduction, magnetic work, and energy storage.

In each AMR cycle, the fluid is assumed to enter the packed bed with a constant temperature T_{hot} at the hot end during the hot-to-cold blow, and T_{cold} at the cold end during cold-to-hot blow, synchronized with a periodically varying magnetic field. The temperature span is $\Delta T = T_{hot} - T_{cold}$ and the heating and cooling powers are

$$Q_h = \int |\dot{m}|_f (h_{f,x=0} - h_{f,T_{hot}}) dt \quad \text{when } \dot{m} < 0, \quad (4)$$

$$Q_c = \int |\dot{m}|_f (h_{f,T_{cold}} - h_{f,x=L}) dt \quad \text{when } \dot{m} > 0, \quad (5)$$

where $h_{f,x=0}$ and $h_{f,x=L}$ are the specific enthalpies of the fluid flowing out of the hot and cold end; $h_{f,T_{hot}}$ and $h_{f,T_{cold}}$ are the specific enthalpies of the fluid at T_{hot} and T_{cold} .

In the numerical model, the central difference and implicit time schemes are used for discretizing the partial differential equations presented above in both space and time. By solving the coupled discretized equations, the temperature gradient can be calculated after each time step given an initial condition, and the model will output the performance indices after reaching the steady state with a tolerance. The main modeling parameters are presented in Table I. The regenerator geometry is kept fixed as a packed bed, and the number of layers, the material, the averaged mass flow rate, as well as the temperature span vary in different cases.

For modeling multi-layer regenerators using $\text{La}(\text{Fe,Mn,Si})_{13}\text{H}_y$, the magnetocaloric properties, mainly the entropy data as a function of the internal magnetic field and temperature, of numerous materials with different T_C are needed. However, existing measurements are limited. Based on the observation that $\text{La}(\text{Fe,Mn,Si})_{13}\text{H}_y$ materials behave quite similarly under the magnetization process and the peaks of both ΔS_{mag} and specific heat c_H are similar in magnitude and shape for a range of T_C ,¹¹ it is assumed that the properties

TABLE I. Main parameters input in the numerical model.

Parameter	Value	Unit
Maximum applied magnetic field	1.2	T
Cross sectional area	225×10^{-6}	m^2
Length	0.100	m
Frequency	2	Hz
Regenerator bed number	20	...
Bed geometry	Packed sphere bed	...
Sphere diameter	0.0003	m
Porosity	0.36	...
MCM mass	2.01	kg
MCM thermal conductivity	8	W/(mK)
MCM density	7000	kg/m^3

of the materials with different T_C other than the characterized material can be approximated by shifting one group of experimental data according to T_C . The material has a T_C of 305.0 K, and it is provided by Vacuumschmelze GmbH, Germany. The measured data of the specific heat at zero field and the absolute value of ΔS_{mag} presented in Fig. 1 are obtained from the Lake Shore 7407 Vibrating Sample Magnetometer (VSM) and a Differential Scanning Calorimeter (DSC) at the Technical University of Denmark.¹⁷ The density of $\text{La}(\text{Fe},\text{Mn},\text{Si})_{13}\text{H}_y$ is measured in a X-ray Diffraction (XRD). The thermal conductivity k_r of $\text{La}(\text{Fe},\text{Mn},\text{Si})_{13}\text{H}_y$ is assumed as 8 W/(mK), which is close the measured k_r data of LaFeSi and LaFeSiH at the ambient temperature.⁹

III. RESULTS AND DISCUSSION

A. Impact of layer number and sensitivity to working temperature

Compared to second order materials, a distinguishing feature of first order materials is the shape of the ΔS_{mag} curves with respect to temperature. The sharp peak in ΔS_{mag} makes a multi-layer design necessary for regenerators using first order materials. In this section, the impact of the number of layers in the regenerator is quantitatively studied. An N_l -layer regenerator is modeled here while operating over a temperature span of 30 K, and N_l is the number of layers. The material in the n^{th} layer is assumed to have $T_{C,n}$

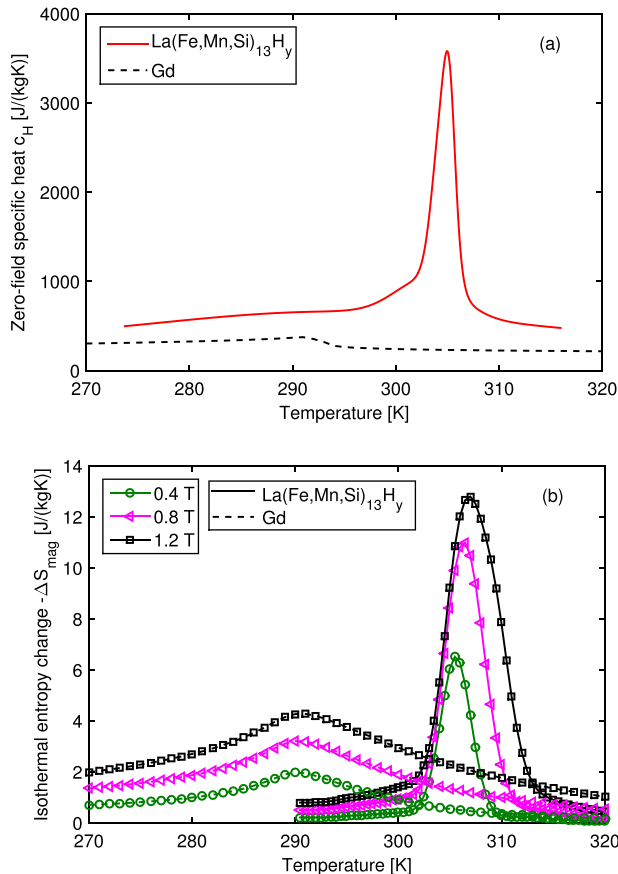


FIG. 1. The specific heat c_H at zero field (a) and the absolute value of isothermal entropy change $-\Delta S_{mag}$ (b) of $\text{La}(\text{Fe},\text{Mn},\text{Si})_{13}\text{H}_y$ and Gd¹⁸ as a function of temperature.

$= 305 - 30(2n - 1)/2n$ ($n = 1, \dots, N_l$). That is, the $T_{C,n}$ follows a linear arrangement along the temperature gradient from 305 to 275 K. Taking a 15-layer regenerator, for example, the $T_{C,n}$ ($n = 1, \dots, 15$) varies from 304 to 276 K with an interval of 2 K according to the expression above.

It is shown in Fig. 1 that the temperature, at which the peak value of ΔS_{mag} occurs, shifts to higher values as the magnetic field increases. Due to this effect, the material is predicted to perform better when the working temperature is higher than the Curie temperature. To estimate the sensitivity to the working temperature, the hot and cold end temperatures (T_{hot} and T_{cold}) are shifted at the same time by -2 to 8 K in the simulation, while the temperature span ΔT is held fixed at 30 K and $T_{C,n} = 305 - 30(2n - 1)/2n$.

Fig. 2 presents the impact of the number of layers N_l and the working temperature T_w on the nominal cooling power $\eta_1 = \frac{Q_{c,T_w,N_l}}{Q_{c,T_w=307-277K,N_l=60}}$, where the denominator $Q_{c,T_w=307-277K,N_l=60}$ is the cooling power of a 60-layer regenerator under T_w of 307–277 K (also the maximum value in the figure) and Q_{c,T_w,N_l} is the cooling power of the N_l -layer regenerator working with a specific T_w . It should be noted that the averaged flow rate is optimized to get the maximum cooling power in each case.

It is shown that the nominal cooling power, η_1 , increases significantly with the number of layers from 4 to 20 and approaches the maximum value when the number of layers exceeds 20 for each working temperature. The maximum number of layers in this study is 60, since a regenerator with more than 60 layers will only lead to a minimal increase in the nominal cooling power according to the results in Fig. 2. 10–15 layers may be practical considering a balance between obtaining the maximum cooling performance and the difficulty of construction. It can be observed that the performance of a multi-layer regenerator is quite sensitive to the absolute working temperature, although the temperature span is fixed. The best T_w is 307–277 K, which is 2 K higher than the

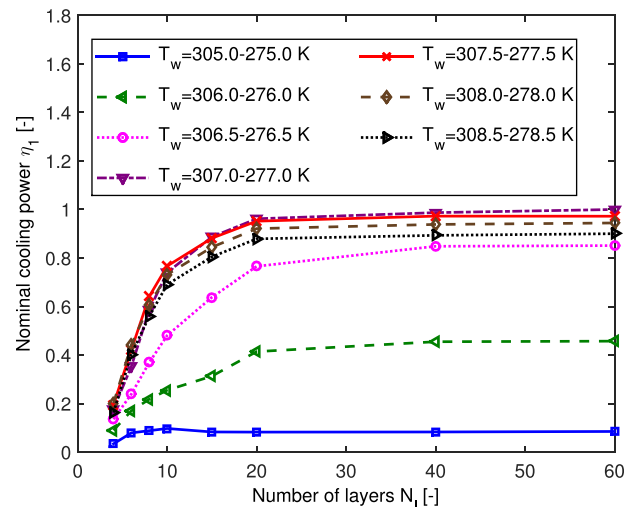


FIG. 2. Impact of number of layers N_l on nominal cooling power $\eta_1 = \frac{Q_{c,T_w,N_l}}{Q_{c,T_w=307-277K,N_l=60}}$ of N_l -layer regenerators with constant temperature span of 30 K.

initially guessed temperature span of 305–275 K. This is explained by the fact that the temperature that corresponds to the peak of ΔS_{mag} rises with increasing magnetic field. The optimal averaged mass flow rate increases with the cooling power, although the data are not presented here.

More detailed results are shown in Fig. 3, and they reveal that the multi-layer regenerators have considerable dependence on the working temperature T_w for fixed $\Delta T = 30$ K. Although both the hot and cold end temperatures are shifted, the horizontal axis only shows the hot end temperature T_{hot} . η_1 reaches the maximum value when T_w is close to 307–277 K and decreases rapidly with changes of T_w to either hot or cold region. Moreover, the nominal cooling power of the multi-layer regenerators decreases much faster when T_w is shifted lower, since the total magneto-caloric effect becomes smaller in a lower T_w region due to the shift of ΔS_{mag} curves. Flat peaks in η_1 curves are observed in the regenerators with fewer layers, which mean the sensitivity is smaller; however, much less nominal cooling power is obtained.

Fig. 4 presents the corresponding results of the coefficient of performance (COP), which is defined as $COP = \frac{Q_c}{Q_h - Q_c}$. Higher COP can be obtained in the regenerators with more layers, and the peak of the COP appears at T_w of 308.5–278.5 K, which is even higher than the guessed temperature region. The results imply that the design of the multi-layer regenerator with the first order materials is challenging, and the number of layers as well as the working temperature should be carefully chosen to achieve desired cooling power and COP.

B. Sensitivity to temperature span ΔT

Another interesting question is how multi-layer regenerators perform under different temperature spans. For the regenerators using the second order materials, the performance curves of cooling power to temperature span in the experiments¹ show a linear shape. However, with the first order materials with a narrow peak in ΔS_{mag} , the multi-layer

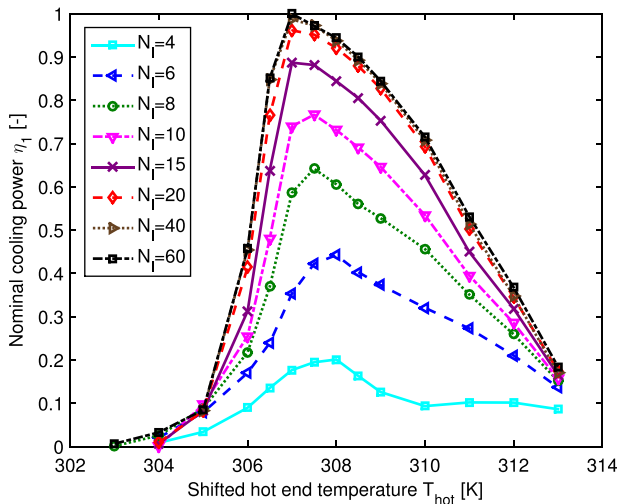


FIG. 3. Impact of working temperature T_w (from T_{hot} to $T_{hot} - 30$ K) on nominal cooling power η_1 of N_l -layer regenerators when temperature span is 30 K.

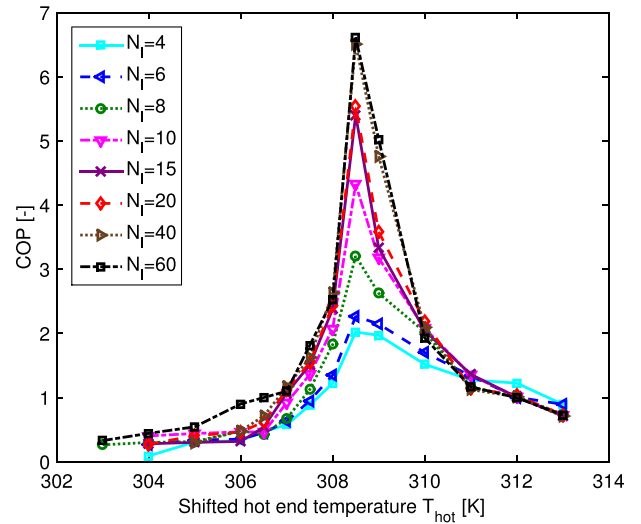


FIG. 4. Impact of working temperature T_w (from T_{hot} to $T_{hot} - 30$ K) on COP of N_l -layer regenerators when temperature span is 30 K.

regenerator, designed for a temperature span of 30 K, probably cannot produce more cooling power when the temperature span is decreased, because in certain layers the material may work outside its respective optimal working temperature.

To investigate this impact, the N_l -layer ($N_l = 4 - 60$) regenerators with $T_{C,n} = 305 - 30(2n - 1)/2n$ K ($n = 1, \dots, N_l$) are chosen as the simulation targets. The hot end temperature T_{hot} is fixed at 308 K, which is close to the optimal value for most cases as found in the previous study; whereas the cold end temperature T_{cold} is varied from 278 K to 298 K with an interval of 5 K, corresponding to temperature spans ΔT from 30 K to 10 K.

The results illustrated in Fig. 5 show the impact of ΔT on nominal cooling power $\eta_2 = \frac{Q_{c,\Delta T,N_l}}{Q_{c,\Delta T=10K,N_l=60}}$ of the N_l -layer regenerators. Although the temperature span is decreased, the increment in the nominal cooling power η_2 is much smaller compared to the behaviors of the regenerators using

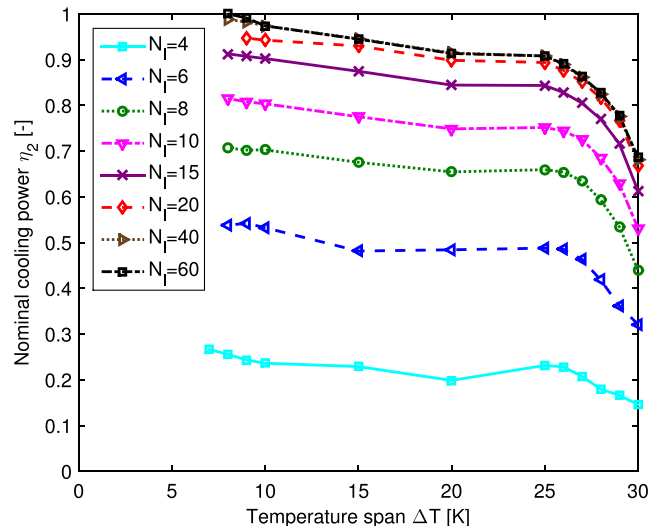


FIG. 5. Impact of temperature span ΔT on nominal cooling power $\eta_2 = \frac{Q_{c,\Delta T,N_l}}{Q_{c,\Delta T=10K,N_l=60}}$ of N_l -layer regenerators with a fixed $T_{C,n}$ arrangement of $305 - 30(2n - 1)/2n$.

Gd.¹ It should be noted that there is a limited temperature range for the measured material properties used in these simulations. In this case, when the temperature span falls below 7 K, the material with the lowest Curie temperature starts to operate outside of the measured property range. Here, the simulations are no longer valid and the corresponding points are not shown in Fig. 5. The results also agree well with the findings presented by Jacobs *et al.*² where similar performance curves can be observed for a refrigerator using a 6-layer regenerator was studied.

Moreover, to account for different temperature spans, the N_I -layer regenerators can be optimized by fitting the Curie temperature of each layer to the specific temperature span ΔT , that is, $T_{C,n} = 305 - \Delta T(2n - 1)/2n$. This means that a different regenerator is modeled for each temperature span. The results of the nominal cooling power for each temperature span $\eta_3 = \frac{Q_{c,\Delta T,N_I}}{Q_{c,\Delta T=5K,N_I=60}}$, where $Q_{c,\Delta T,N_I=60}$ is the cooling power of a 60-layer regenerator over the temperature span of ΔT , are presented in Fig. 6. The impact of the layer number is similar to the results in Fig. 2; however for a smaller temperature span, the regenerators reach the maximum cooling performance much faster, meaning fewer layers are needed to reach a cooling power near the maximum. This is because the ΔS_{mag} curves for each material have a certain width of best working temperature region and fewer layers are needed to cover a smaller temperature span.

The inset in Fig. 6 shows the number of layers when the cooling power reaches 90% of the maximum value ($\eta_3 = 0.9$) as a function of temperature span. The curve shows an approximately linear relation and gives a slope of 2.24 layers per 5 K temperature span, which can be used as a reference for choosing the number of layers when constructing layered regenerators with La(Fe,Mn,Si)₁₃H₉.

The results of the nominal cooling power $\eta_4 = \frac{Q_{c,\Delta T,N_I}}{Q_{c,\Delta T=5K,N_I=60}}$ produced by the multi-layer regenerators with optimized $T_{C,n}$ arrangement are presented in Fig. 7. The performance curves of the N_I -layer regenerators now behave in

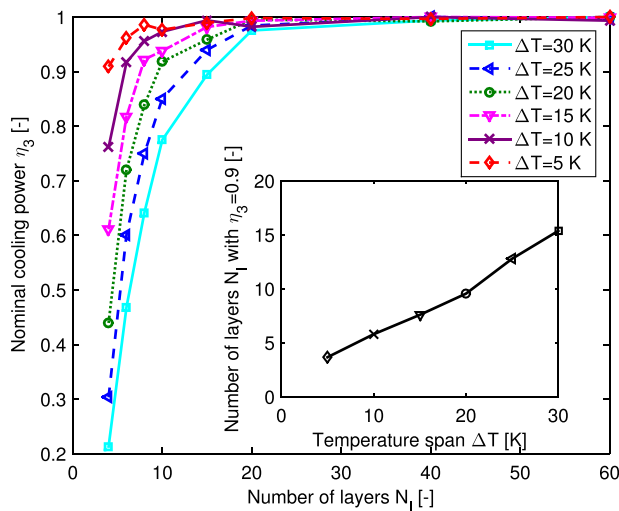


FIG. 6. Impact of number of layers N_I on nominal cooling power $\eta_3 = \frac{Q_{c,\Delta T,N_I}}{Q_{c,\Delta T=5K,N_I=60}}$ of N_I -layer regenerators with optimized $T_{C,n}$ arrangement of $305 - \Delta T(2n - 1)/2n$.

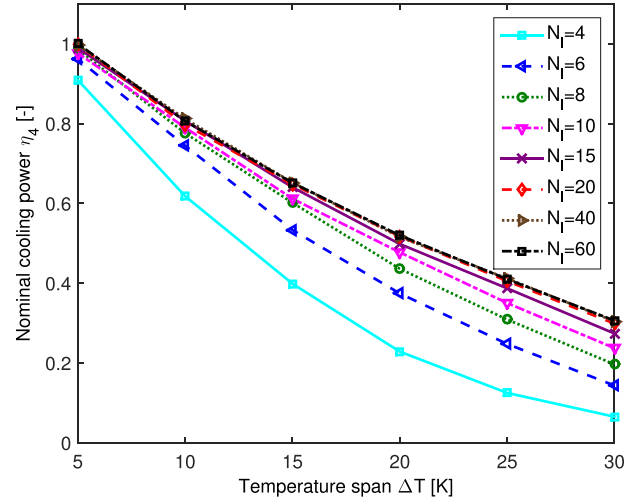


FIG. 7. Impact of temperature span ΔT on nominal cooling power $\eta_4 = \frac{Q_{c,\Delta T,N_I}}{Q_{c,\Delta T=5K,N_I=60}}$ of N_I -layer regenerators with optimized $T_{C,n}$ arrangement of $305 - \Delta T(2n - 1)/2n$.

a more linear manner, which is different than those with fixed $T_{C,n}$ arrangement shown in Fig. 5. The curves split out when the temperature span becomes larger, meaning that more layers are needed to approach the maximum performance, which also reflects the conclusions drawn before.

C. Impact of Curie temperature variation in specific positions

There will always be some manufacturing variation in the Curie temperature T_C for the materials studied here, meaning the ideal T_C arrangement is quite difficult to achieve. The effect of Curie temperature variation in layered regenerators is not well understood and this will be quantified in the following study. A straightforward way to investigate this is to study the impact of the variation in the Curie temperature $\Delta T_{C,n}$, which is $T_{C,n,real} - T_{C,n,base}$ in the n^{th} layer. $T_{C,n,real}$ and $T_{C,n,base}$ are the real and base Curie temperature of every material for constructing a layered regenerator, and positive $\Delta T_{C,n}$ means shifting $T_{C,n,real}$ of the n^{th} layer to a higher temperature, and vice versa.

In the simulation, a 15-layer regenerator, in which the n^{th} layer has the Curie temperature $T_{C,n,base} = 305 - 30(2n - 1)/2n$ K ($n = 1 \dots 15$), is used as the baseline for comparison, and in this case $\Delta T_{C,n} = 0$. Then one at a time, $T_{C,n}$ of every individual layer in the 15-layer regenerator is shifted by the variation $\Delta T_{C,n}$, which is considered to vary from -1.6 to 1.6 K with a step of 0.4 K. The temperature span is held constant at $307-277$ K, and it is close to the best working temperature according to the previous study. As the number of layers and the working temperature are fixed, the optimal averaged mass flow rate for each case is close to each other, and a constant value is used in the rest of this study. The impact of $\Delta T_{C,n}$ in a single layer- n is shown in Fig. 8. The nominal cooling power $\eta_5 = \frac{Q_{c,\Delta T_{C,n}}}{Q_{c,\Delta T_{C,n}=0}}$, where $Q_{c,\Delta T_{C,n}=0}$ is the cooling power of the base regenerator with $\Delta T_{C,n} = 0$, meaning an even Curie temperature arrangement, and $Q_{c,\Delta T_{C,n}}$ is the cooling power of a regenerator with certain $\Delta T_{C,n}$ in the n^{th} layer. For most cases, the maximum value of η_5 is close

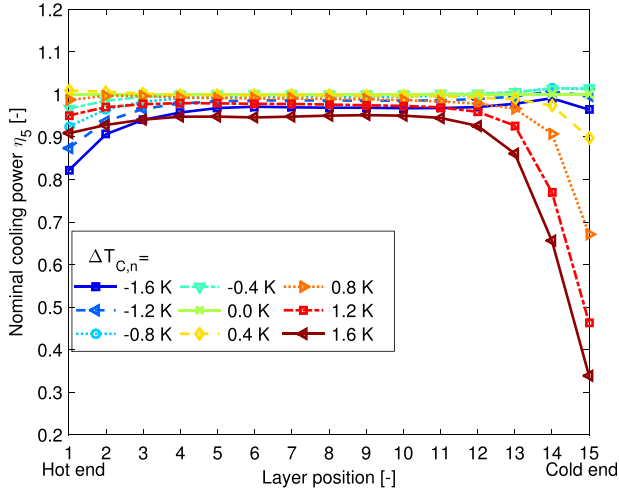


FIG. 8. Impact of Curie temperature variation $\Delta T_{C,n}$ of every individual layer on nominal cooling power $\eta_5 = \frac{Q_c \Delta T_{C,n}}{Q_c \Delta T_{C,n=0}}$.

to 1, which shows that the base regenerator with $\Delta T_{C,n} = 0$ is the best choice, that is, an even Curie temperature arrangement produces a cooling power close to the maximum value. It can be seen that the performance is most sensitive to $\Delta T_{C,n}$ for the cases of shifting the layers close to the hot or cold ends. Especially when shifting the layer-13, 14, and 15 to the hot region, η_5 decreases dramatically, which means that the regenerators are more sensitive to $\Delta T_{C,n}$ in the layers close to the cold end.

D. Impact of Curie temperature variations following statistical distributions

To reflect the impact of production uncertainties, it is necessary to model layered regenerators where the Curie temperature $T_{C,n}$ of each layer may vary according to a uniform distribution or a normal distribution; the latter is expected to be closer to reality. Therefore, in this section, the acceptable degree of the Curie temperature variation $\Delta T_{C,n}$ is investigated by running a batch of simulations and reflecting on the range of AMR performance that can arise from

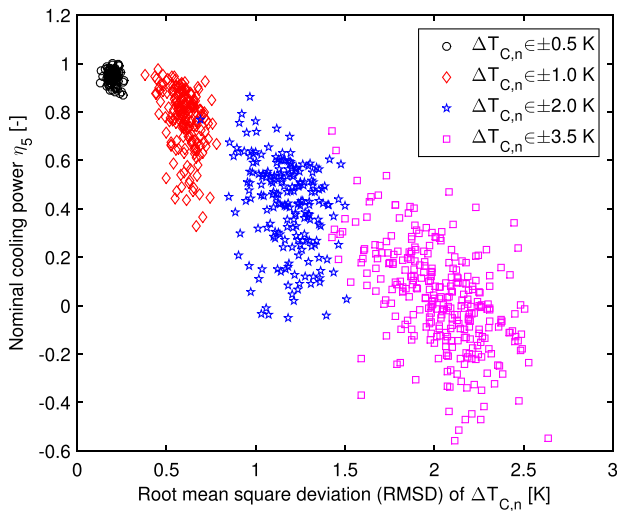


FIG. 9. Impact of *RMSD* of $\Delta T_{C,n}$ on nominal cooling power η_5 when $\Delta T_{C,n}$ follows a uniform distribution.

assuming $\Delta T_{C,n}$ to be a stochastic variable. The method used to generate the new regenerators assumes that the $\Delta T_{C,n}$ follows a uniform distribution first. The base regenerator is still the one presented in Sec. III C, and each layer of the new 15-layer regenerator has a random shift that is modeled in four magnitudes: ± 0.5 , ± 1 , ± 2 , and ± 3.5 K. The uniform distribution makes sure the probability that $\Delta T_{C,n}$ of each layer appears inside the defined region is the same. For each magnitude, 200 such combinations are generated randomly and the nominal cooling powers are compared. The root mean square deviation $RMSD = \sqrt{\frac{\sum_{n=1}^{15} \Delta T_{C,n}^2}{15}}$ is utilized to present the degree of overall variation in $T_{C,n}$. *RMSD* close to 0 means near to the even $T_{C,n}$ arrangement, conversely large values mean higher average degrees of variation in $T_{C,n}$, in other words, uneven $T_{C,n}$ arrangement.

Fig. 9 shows four groups of data and the markers represent different magnitudes. Here, negative nominal cooling power is still presented for statistical purposes. It can be seen that the maximum nominal cooling power η_5 is close to 1 and η_5 decreases rapidly with the *RMSD* of $\Delta T_{C,n}$ in total, which means the regenerators can only tolerate relatively small $\Delta T_{C,n}$ on the order of ± 0.5 K without significant loss in cooling power. With a variation larger than ± 1 K, η_5 is away from the median value, which implies that larger variation adds considerable difficulty to realize designed cooling power of the multi-layer regenerators in the real construction.

In the following studies, we present the sensitivity of the multi-layer regenerators when $\Delta T_{C,n}$ follows a normal distribution with a mean value μ and standard deviation σ . In the simulations, $\mu = 0$ and σ is set from 0.3 K to 3 K with steps of 0.3 K. For each σ , 200 regenerators are simulated (in total 2000 cases). The results of the nominal cooling power are presented in Fig. 10. It can be seen that the impact of σ is significant. For $\sigma = 0.3$ K, the median value of the nominal cooling power is 0.960, and the 25%–75% box shows the

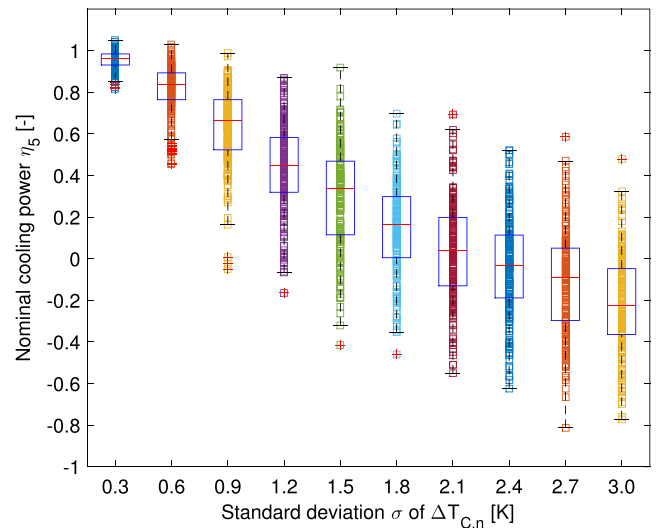


FIG. 10. Impact of standard deviation σ of $\Delta T_{C,n}$ on nominal cooling power η_5 when $\Delta T_{C,n}$ follows a normal distribution. The central mark of the 25%–75% box is the median value of η_5 for each σ , and the edges of the box are the 25th and 75th percentiles. The whiskers show the most extreme data points without outliers, and the outliers are plotted individually in red cross.

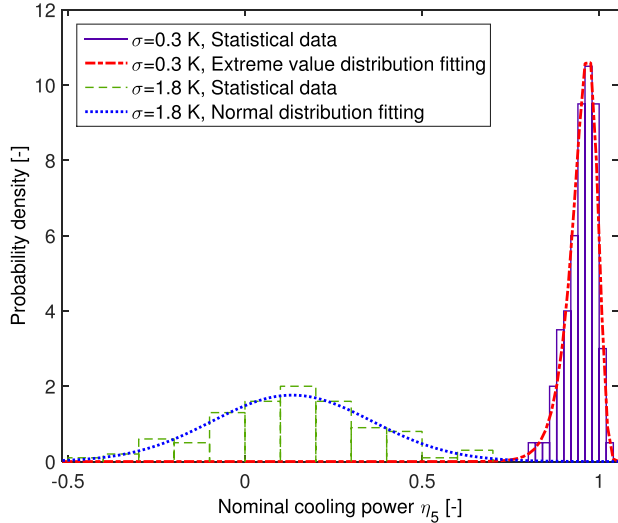


FIG. 11. Distribution fittings of statistical data of nominal cooling power η_5 when $\sigma = 0.3$ K and $\sigma = 1.8$ K. For $\sigma = 0.3$ K, the expectation and standard variation of η_5 are $\mu_{\eta_5} = 0.969$ and $\sigma_{\eta_5} = 0.034$; for $\sigma = 1.8$ K, they are $\mu_{\eta_5} = 0.133$ and $\sigma_{\eta_5} = 0.226$.

upper limit of 0.984 and the low limit of 0.931, which implies that the regenerator performance will lie in this region with a probability of 50%. However, with increasing σ , the median value decreases dramatically and the 25%–75% box becomes bigger, meaning there is larger uncertainty in η_5 . It can be seen that $\sigma > 0.6$ K will lead to at least 16.6% performance reduction in the median value and η_5 varies in quite a large range, which means a risk of getting vastly different performance from two regenerators built in the same way.

Fig. 11 presents the histogram and probability density of η_5 when $\sigma = 0.3$ K and $\sigma = 1.8$ K. It can be observed that in each case η_5 follows the extreme value distribution and the normal distribution, respectively. Besides the obvious difference in median values, the case $\sigma = 0.3$ K shows a concentrated distribution and there is a much smaller calculated

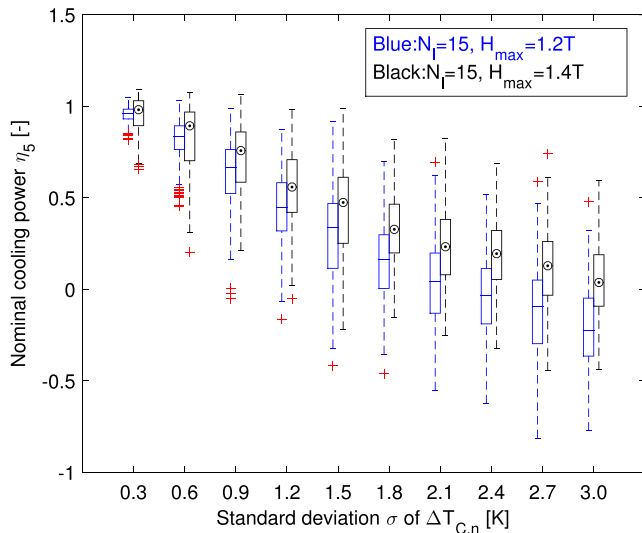


FIG. 12. Sensitivity of nominal cooling power η_5 to standard deviation σ of $\Delta T_{C,n}$ with $H_{\max} = 1.2$ T and $H_{\max} = 1.4$ T. The line inside the box represents the median value of η_5 when $H_{\max} = 1.2$ T, and the spot for $H_{\max} = 1.4$ T.

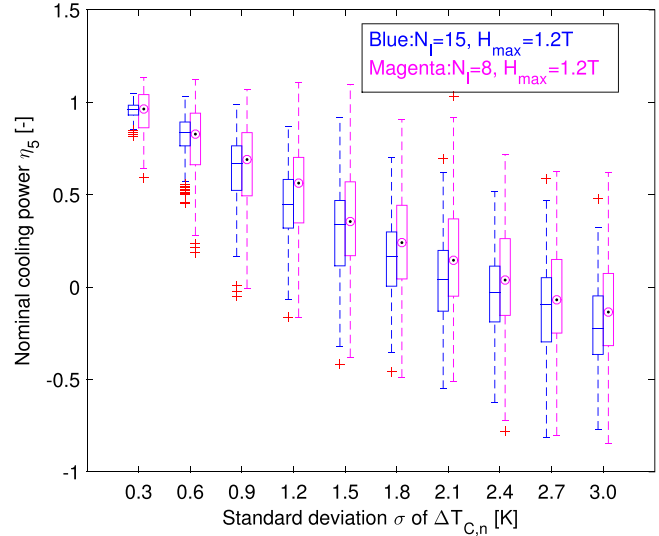


FIG. 13. Sensitivity of nominal cooling power η_5 to standard deviation σ of $\Delta T_{C,n}$ with $N_l = 15$ and $N_l = 8$. The line inside the box represents the median value of η_5 when $N_l = 15$, and the spot for $N_l = 8$.

standard deviation in the nominal cooling power σ_{η_5} of 0.034, compared to $\sigma_{\eta_5} = 0.226$ of the wide distribution when $\sigma = 1.8$ K. It is also reflected in Fig. 10 in the type of wider box and region of extreme values.

As the ΔS_{mag} curve tends to be wider when the internal magnetic field increases, it is hypothesized that the multi-layer regenerators should be less sensitive to Curie temperature variation $\Delta T_{C,n}$ with a larger applied field. This is verified in Fig. 12. The results from the maximum applied field of 1.2 T and 1.4 T are compared, and it shows that not only the median cooling power is higher at larger σ but also the variation of the nominal cooling power is lower at higher applied field, that is, the regenerators become less sensitive to σ with an increase of the maximum applied field from 1.2 T to 1.4 T.

The sensitivity of an 8-layer regenerator is also investigated. Fig. 13 shows that the median value of η_5 from the 8-layer regenerator has a smaller slope with increasing σ compared to that of the 15-layer regenerators; however, the deviation in the nominal cooling power becomes larger, which indicates the regenerators with more layers are less sensitive and can reduce the risk of the performance degradation. It should be noted that, generally, the regenerators with more layers and larger maximum applied field will produce more cooling power; therefore, the base values for calculating η_5 in Figs. 12 and 13 are different.

IV. CONCLUSION

Multi-layer regenerators using the first order material series $\text{La}(\text{Fe}, \text{Mn}, \text{Si})_{13}\text{H}_y$ were investigated. The impact of the number of layers N_l , the sensitivity to the working temperature T_w , and the sensitivity to the variations in the Curie temperature $\Delta T_{C,n}$ were presented. The results showed that the nominal cooling power increases significantly with N_l , and from a practical point, around 10 to 15 layers may be suitable for a temperature span ΔT of 30 K given an applied field of

1.2 T. Meanwhile, multi-layer regenerators are quite sensitive to T_w and the best temperature region is 307–277 K. With a non-optimized $T_{C,n}$ arrangement, the performance increases slowly with decreasing ΔT . It was also shown that fewer layers are needed for a smaller ΔT with optimized $T_{C,n}$ arrangement, and around 2.24 layers are necessary for every 5 K ΔT to get 90% of the maximum performance.

Moreover, Curie temperature variations $\Delta T_{C,n}$ in the layers close to the cold or hot end have significant impact on the system performance, which is most sensitive to $\Delta T_{C,n}$ of layers close to the cold end. Furthermore, AMR performance with $\Delta T_{C,n}$ that varies according to a uniform or normal distribution was predicted for a population of randomly generated layers. The results showed that multi-layer regenerators are considerably sensitive to RMSD of $\Delta T_{C,n}$ for a uniform distribution, and the standard deviation σ of $\Delta T_{C,n}$ for a normal distribution. In the latter case, $\sigma > 0.6$ K will cause at least 16.6% decrease in the median value of the nominal cooling power η_5 and increase in the uncertainty of η_5 , which implies that there may be huge difference in the performance of two regenerators built from materials with the same accuracy in Curie temperature. It is also predicted that larger applied field and layer number will decrease the sensitivity of the multi-layer regenerator to $\Delta T_{C,n}$.

ACKNOWLEDGMENTS

This work was financed by the ENOVHEAT project which is funded by Innovation Fund Denmark (Contract No. 12-132673). The authors would like to thank Vacuumschmelze GmbH, Germany for providing the $\text{La}(\text{Fe},\text{Mn},\text{Si})_{13}\text{H}_y$ material.

- ¹K. Engelbrecht, D. Eriksen, C. R. H. Bahl, R. Bjørk, J. Geyti, J. A. Lozano, K. K. Nielsen, F. Saxild, A. Smith, and N. Pryds, "Experimental results for a novel rotary active magnetic regenerator," *Int. J. Refrig.* **35**, 1498–1505 (2012).
- ²S. Jacobs, J. Auringer, A. Boeder, J. Chell, L. Komorowski, J. Leonard, S. Russek, and C. Zimm, "The performance of a large-scale rotary magnetic refrigerator," *Int. J. Refrig.* **37**, 84–91 (2014).
- ³S. Y. Dan'Kov, A. Tishin, V. Pecharsky, and K. Gschneidner, "Magnetic phase transitions and the magnetothermal properties of gadolinium," *Phys. Rev. B* **57**, 3478–3490 (1998).
- ⁴J. A. Barclay, "The theory of an active magnetic regenerative refrigerator," NASA STI/Recon Technical Report No. 83 (1982), p. 34087.
- ⁵J. Tušek, A. Kitanovski, U. Tomc, C. Favero, and A. Poredoš, "Experimental comparison of multi-layered LaFeCoSi and single-layered Gd active magnetic regenerators for use in a room-temperature magnetic refrigerator," *Int. J. Refrig.* **37**, 117–126 (2014).
- ⁶A. Rowe and A. Tura, "Experimental investigation of a three-material layered active magnetic regenerator," *Int. J. Refrig.* **29**, 1286–1293 (2006).
- ⁷A. Rowe, "Thermodynamics of active magnetic regenerators: Part I," *Cryogenics* **52**, 111–118 (2012).
- ⁸K. Engelbrecht, K. K. Nielsen, C. R. H. Bahl, C. P. Carroll, and D. van Asten, "Material properties and modeling characteristics for $\text{MnFeP}_{1-x}\text{As}_x$ materials for application in magnetic refrigeration," *J. Appl. Phys.* **113**, 173510 (2013).
- ⁹S. Fujieda, Y. Hasegawa, A. Fujita, and K. Fukamichi, "Thermal transport properties of magnetic refrigerants $\text{La}(\text{Fe}_x\text{Si}_{1-x})_{13}$ and their hydrides, and $\text{Gd}_5\text{Si}_2\text{Ge}_2$ and MnAs ," *J. Appl. Phys.* **95**, 2429–2431 (2004).
- ¹⁰A. Barcza, M. Katter, V. Zellmann, S. Russek, S. Jacobs, and C. Zimm, "Stability and magnetocaloric properties of sintered $\text{La}(\text{Fe},\text{Mn},\text{Si})\text{H}$ alloys," *IEEE Trans. Magn.* **47**, 3391–3394 (2011).
- ¹¹K. Morrison, K. Sandeman, L. Cohen, C. Sasso, V. Basso, A. Barcza, M. Katter, J. Moore, K. Skokov, and O. Gutfleisch, "Evaluation of the reliability of the measurement of key magnetocaloric properties: A round robin study of $\text{La}(\text{Fe},\text{Mn},\text{Si})\text{H}$ conducted by the SSEE consortium of European laboratories," *Int. J. Refrig.* **35**, 1528–1536 (2012).
- ¹²A. Fujita, S. Fujieda, Y. Hasegawa, and K. Fukamichi, "Itinerant-electron metamagnetic transition and large magnetocaloric effects in $\text{La}(\text{Fe}_x\text{Si}_{1-x})_{13}$ compounds and their hydrides," *Phys. Rev. B* **67**, 104416 (2003).
- ¹³C. Wang, Y. Long, T. Ma, B. Fu, R. Ye, Y. Chang, F. Hu, and J. Shen, "The hydrogen absorption properties and magnetocaloric effect of $\text{La}_{0.8}\text{Ce}_{0.2}(\text{Fe}_{1-x}\text{Mn}_x)_{11.5}\text{Si}_{1.5}\text{H}_y$," *J. Appl. Phys.* **109**, 07A910 (2011).
- ¹⁴A. Smith, C. R. H. Bahl, R. Bjørk, K. Engelbrecht, K. K. Nielsen, and N. Pryds, "Materials challenges for high performance magnetocaloric refrigeration devices," *Adv. Energy Mater.* **2**, 1288–1318 (2012).
- ¹⁵T. Lei, K. K. Nielsen, and K. Engelbrecht, "Modelling and simulation of regenerators with complex flow arrangements for active magnetocaloric refrigeration," in *ASME 12th Biennial Conference on Engineering Systems Design and Analysis* (2014), Vol. 3, p. V003T12A007.
- ¹⁶K. K. Nielsen, G. Nellis, and S. Klein, "Numerical modeling of the impact of regenerator housing on the determination of Nusselt numbers," *Int. J. Heat Mass Transfer* **65**, 552–560 (2013).
- ¹⁷S. Jeppesen, S. Linderroth, N. Pryds, L. T. Kuhn, and J. B. Jensen, "Indirect measurement of the magnetocaloric effect using a novel differential scanning calorimeter with magnetic field," *Rev. Sci. Instrum.* **79**, 083901 (2008).
- ¹⁸R. Bjørk, C. R. H. Bahl, and M. Katter, "Magnetocaloric properties of $\text{LaFe}_{13-x-y}\text{Co}_x\text{Si}_y$ and commercial grade Gd," *J. Magn. Magn. Mater.* **322**, 3882–3888 (2010).